

# Universal scaling of optimal current distribution in transportation networks

Filippo Simini,<sup>1,\*</sup> Andrea Rinaldo,<sup>2,†</sup> and Amos Maritan<sup>1,‡</sup>

<sup>1</sup>*Dipartimento di Fisica “Galileo Galilei,” CNISM and INFN, Università di Padova, via Marzolo 8, 35131 Padova, Italy*

<sup>2</sup>*ECHO/ISTE/ENAC, Ecole Polytechnique Fédérale, 1015 Lausanne, Switzerland*

(Received 23 August 2008; revised manuscript received 13 February 2009; published 29 April 2009)

Transportation networks are inevitably selected with reference to their global cost which depends on the strengths and the distribution of the embedded currents. We prove that optimal current distributions for a uniformly injected  $d$ -dimensional network exhibit robust scale-invariance properties, independently of the particular cost function considered, as long as it is convex. We find that, in the limit of large currents, the distribution decays as a power law with an exponent equal to  $(2d-1)/(d-1)$ . The current distribution can be exactly calculated in  $d=2$  for all values of the current. Numerical simulations further suggest that the scaling properties remain unchanged for both random injections and by randomizing the convex cost functions.

DOI: 10.1103/PhysRevE.79.046110

PACS number(s): 89.75.Hc, 89.75.Da, 89.75.Fb, 89.75.Kd

## I. INTRODUCTION

Finding efficient ways of distributing (or collecting) matter injected through a given region, spanned, e.g., by a regular lattice, from (at) a unique source (sink) is relevant to a variety of problems arising both for natural and artificial systems. The main mechanisms that are known to achieve a capillary distribution are by diffusion or through a network-like structure providing a near uniform spatial supply (drainage), or a combination of them. Network arrangements, of this kind, are observed in many living organisms, like for instance circulatory and lymphatic systems in animals or xylem and roots in vascular plants, and are also widely employed in artificial systems such as electrical or hydraulic transmissions and fluvial basins [1–5].

Certainly, one wonders what is the basic selection principle that favors, say, treelike versus looping network structures, in view of the widespread occurrence of both forms in nature and elsewhere [6,7] [5]. To that end, it has been previously shown that treelike structures emerge as local minima of global energy expenditure in networks whose transportation cost is physically constrained to be a concave function, such as in the case of river networks [8].

Transportation costs generally depend on the strength of currents and on network topology. The best known example is the electrical resistor network [9,10]: consider a square lattice where a resistor is placed at every bond between each pair of nearest-neighbor nodes. Each node is externally supplied by a unit flux. If a sink collects all the currents, one is capable of controlling the current fluxes in all bonds by assigning the potential differences between pairs of nodes. The total cost in the transportation—the dissipated power—is proportional by Ohm’s law to the sum of the square of currents:  $\mathcal{E}(\{I_b\}) = \sum_b |I_b|^2$ . Optimal resistor networks are thus obtained by setting the potentials in order to minimize the total transportation cost. The most immediate way to generalize the resistor network case is to replace the exponent “2” by a generic exponent  $\gamma > 0$ .

The case  $\gamma \leq 1$  has been characterized exactly [4,8,11–13]. It was shown there that the cost function admits many local minima corresponding to configurations with currents present only on the bonds of spanning trees [8]. The case  $\gamma = 1/2$  exhibits scaling behavior akin to river networks [4,11,12,14].

The case  $\gamma = 1$  is related to the Voter model [15], mass aggregation [16–19], directed sandpile models [20], and Kleiber’s law of metabolic scaling of living organism [21]. Recently optimal transportation networks with a global constraint have been studied in a variety of contexts [22,23], where different topologies of the optimal transportation network arising in the cases  $\gamma < 1$  and  $\gamma > 1$  have been investigated also by Bohm and Magnasco [23].

The case  $\gamma > 1$  is an example of convex transportation costs. Important real-world examples are found, for example, in road traffic analyses where more cars cause disproportionately higher costs (travel times), usually modeled as convex functions or in any electricity distribution network owing to Ohm’s law. Convex cost functions also occur in many operations research applications as pointed out in [24].

## II. NUMERICAL RESULTS

Here we address the current distribution for the case corresponding to a general convex cost function of the circulating currents:

$$\mathcal{E}(\{I_b\}) = \sum_b E(|I_b|), \quad (1)$$

where the sum spans all network bonds  $b$ . In specific examples and numerical simulations we will consider the particular class of convex functionals with  $E(|I_b|) = |I_b|^\gamma / \gamma$  and  $\gamma > 1$ . It will be shown, however, that our findings are valid for an arbitrary convex cost function  $E$  with finite first derivative which depends only on current strength. Notice that for a nonlinear resistor network the transportation cost  $\mathcal{E}$  is proportional to the dissipated power only for the case  $E(|I_b|) \propto |I_b|^\gamma$ , as discussed in [25,26]. We will focus here only on finite networks. The goal is to determine the current probability distribution corresponding to the current configuration  $\{I_b\}$ , which minimizes the total transportation cost  $\mathcal{E}$  in

\*simini@pd.infn.it

†andrea.rinaldo@epfl.ch

‡maritan@pd.infn.it

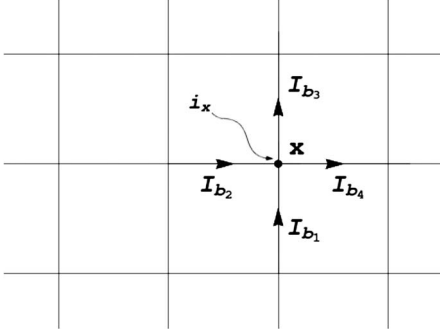


FIG. 1. The current conservation at node  $x$ . The sum of all currents flowing into node  $x$  must be equal to the sum of currents flowing out of node  $x$ :  $I_{b_1} + I_{b_2} - I_{b_3} - I_{b_4} + i_x = 0$ .

the large size limit and its scaling behavior as a function of the cost  $E(|I|)$ .

The minimization of  $\mathcal{E}$  is subject to the local constraints of current conservation at each node  $x$ : the sum of all currents flowing into a node, taken as negative (positive) if directed outward (inward), must equal the injected nodal flux,  $i_x$  (see Fig. 1). Because such constraint is linear in the  $I_b$ s, if  $\mathcal{E}$  is a convex function then it admits a single global minimum. The existence and uniqueness of the solution for infinite networks have been addressed elsewhere [25].

As shown below, we find quite generally that the cumulative probability distribution function (CPDF), i.e., the fraction of currents  $|I_b|$  larger than  $I$ , obeys the finite-size scaling

$$P_c(I|L) = F\left(\frac{I}{L}\right) \quad \forall d, \gamma > 1, \quad I \geq 0, \quad (2)$$

where  $L$  is the linear size of the system and  $F$  is the scaling function which at large  $x$  behaves as  $F(x) \sim x^{1-\tau}$  with  $\tau = (2d-1)/(d-1)$  and  $\lim_{x \rightarrow 0} F(x) = 1$ . This scaling form holds independently of the particular convex cost function considered. The standard scaling behavior for the case  $E(|I_b|) = |I_b|^\gamma / \gamma$  and  $\gamma \leq 1$  [11,27] corresponding to a nonconvex cost function was instead found to be

$$P_c(I|L) = I^{1-\tau} f\left(\frac{I}{L^d}\right) \quad \gamma < 1, \quad I \geq 1 \quad (3)$$

with  $\lim_{x \rightarrow 0} f(x) = \text{const}$ , i.e., a pure power law is obtained in the large size limit ( $\tau = 1.43 \pm 0.03$  in  $d=2$  and  $\gamma=1/2$ ). The  $\gamma=1$  case was solved exactly in all dimensions using a mapping to reaction diffusion models [16] and  $\tau = 2(d+1)/(d+2)$  when the dimensionality is lower than the upper critical dimension,  $d_c=2$ , and  $\tau=3/2$  when  $d > 2$ . In the present case no upper critical dimension is found above which the exponent remains the same.

Let us first describe the results of the numerical determination of current configuration minimizing Eq. (1) with  $E(|I_b|) = |I_b|^\gamma$  and  $\gamma > 1$  in a square lattice (i.e.,  $d=2$ ) of linear size  $L$  where a uniform input at each site  $i_x=1$  is assumed (at the sink where all currents are collected one has  $i_{\text{sink}} = -L^2 + 1$ ). We have used open boundary conditions for simplicity because we do not expect that they influence the scaling behavior in the large size limit. Because our problem reduces

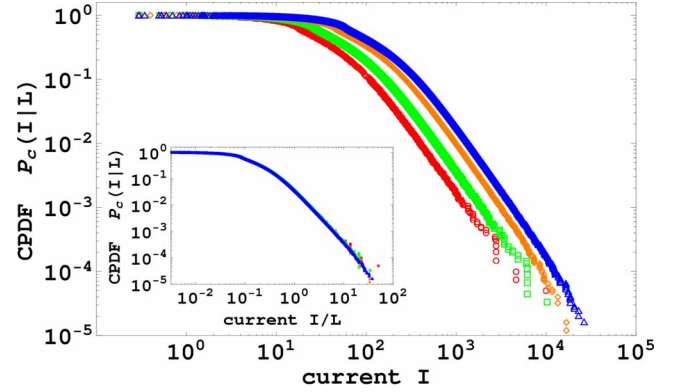


FIG. 2. (Color online) CPDF for square lattices of different sizes [ $L=201$  (red circles), 301 (green squares), 501 (orange rhombi), 701 (blue triangles)] and for  $\gamma=2$  (on log-log scale). Fitting the tail of the distribution with a power law yields a value for the exponent  $\tau \approx 3$ , e.g., for  $L=301$  we get  $\tau = 2.975 \pm 0.045$  (the exponent of the power law was estimated using the method of maximum likelihood [29,30], and the error was calculated with the bootstrap method [31]). In the inset we plot  $P_c(I|L)$  vs  $I/L$ , for all  $L$ 's and  $I$ 's considered above. The collapse of the curves indicates that the CPDF is a function of the ratio  $I/L$ .

to the minimization of a convex function of many variables, we have used the nonlinear conjugate gradient method [28]. The CPDF,  $P_c(I|L)$ , is plotted in Fig. 2 for lattices of different sizes  $L$  and for  $\gamma=2$ , the resistor network. It has the following scaling behavior:

$$P_c(I|L) = \begin{cases} \text{const} & \text{for } 0 \leq I \leq L \\ I^{1-\tau} & \text{for } L \leq I \leq L^2, \end{cases} \quad (4)$$

with  $\tau = 2.975 \pm 0.045$ . In the inset of Fig. 2 the CPDF is plotted versus  $I/L$  for various  $L$ , showing that indeed  $P_c(I|L)$  is a homogeneous function of the ratio  $I/L$ .

We have also performed numerical optimizations with different values of  $\gamma > 1$  in  $d=2$ . Figure 3 shows pictures of the optimized current configuration and the corresponding CPDFs are plotted in Fig. 4. Because data overlap, and although the current configuration of global minimum for  $\mathcal{E}$  varies with  $\gamma$  as shown in Fig. 3, it is suggested that the distribution of currents is independent of the exponent  $\gamma$  when  $\gamma > 1$ . Additionally, we performed simulations on a  $2-d$  triangular lattice. The scaling behavior of the CPDF proved to be independent of the underlying lattice's structure.

### III. ANALYTICAL RESULTS

We attack the problem analytically in the continuum limit (this will be justified *a posteriori*). We begin to illustrate the procedure in detail for the case  $E(|I_b|) = |I_b|^\gamma / \gamma$ ; later on we will extend it to the more general case.

Under the assumption that the current distribution, in the large size limit, does not depend on the shape of the volume we enclose our system in a region  $\Omega = \{x: \|x\|_\gamma \leq L\}$ , whose volume will be denoted as  $|\Omega|$ . We have defined the norm as  $\|x\|_\gamma \equiv [\sum_\mu |x_\mu|^\gamma]^{1/\gamma}$ . In the case  $\gamma=2$ ,  $\Omega$  is a sphere of radius  $R \equiv L$ . Let  $\mathbf{j}(\mathbf{x})$  be the current density at location  $\mathbf{x}$  whereas

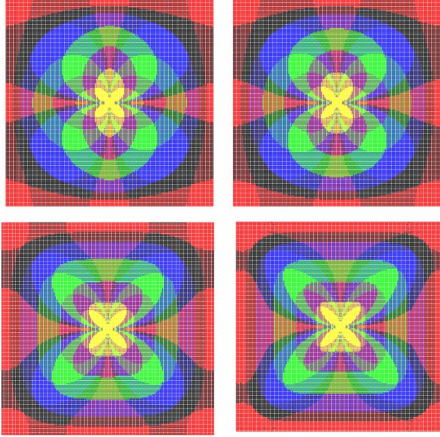


FIG. 3. (Color online) Currents' intensity in the optimal configuration for different values of the exponent  $\gamma$  and for the size  $L = 151$  of a square lattice. From top left to bottom right:  $\gamma = 1.5$ ,  $\gamma = 2$ ,  $\gamma = 4$ , and  $\gamma = 6$ . The petal-like arrangement of currents is not an artifact of the underlying lattice geometry but arises from the decomposition of current vectors into components. The direction of currents is toward the center (directed networks). The colors indicate the intensity of currents: yellow:  $L \leq I$ , purple:  $L/2 \leq I < L$ , green:  $L/4 \leq I < L/2$ , blue:  $L/8 \leq I < L/4$ , black:  $L/16 \leq I < L/8$ , red:  $I < L/16$ .

$i(\mathbf{x}) = i_0[1 - |\Omega| \delta^d(\mathbf{x})]$  is the external input. The Dirac delta distribution  $\delta^d(\mathbf{x})$  [a compact notation for the  $d$ -dimensional notation  $\delta^d(\mathbf{x}) \equiv \delta(x_1) \dots \delta(x_d)$ ] represents the sink at the origin, whereas  $i_0$  is the uniform input. The components  $j_\mu(\mathbf{x})$  ( $\mu = 1, \dots, d$ ) of the vector  $\mathbf{j}(\mathbf{x})$  represent the currents along the positive direction of coordinate axes at position  $\mathbf{x}$ .

In the continuum case we define a cost functional analogous to Eq. (1) as

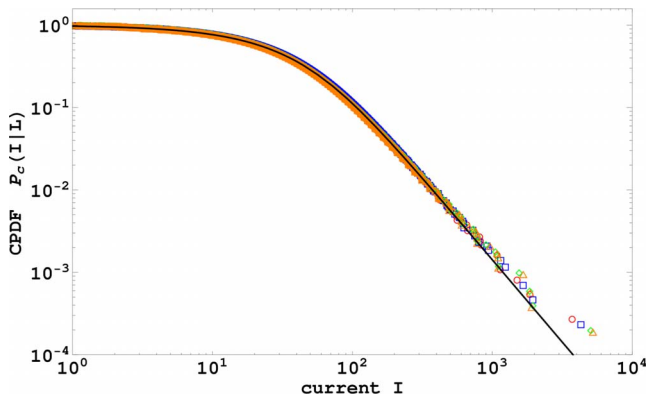


FIG. 4. (Color online) Comparison of CPDFs of global minimum configurations for the class of convex functionals (1) with  $E(|I_b|) = |I_b|^\gamma / \gamma$  and different  $\gamma$  values:  $\gamma = 1.5$  (red circles), 2 (blue squares), 4 (green rhombi), 6 (orange triangles). The black solid line is Eq. (9), the CPDF of the analytic solution of Eq. (6). The shapes of the network boundaries in the various cases are chosen as explained in the text.

$$\mathcal{E} = \int_{\Omega} d^d x \frac{\|\mathbf{j}(\mathbf{x})\|_{\gamma}^{\gamma}}{\gamma}. \quad (5)$$

We search for the current configuration that minimizes the cost function Eq. (5) with the constraint of the current conservation law,  $\nabla \cdot \mathbf{j}(\mathbf{x}) = i(\mathbf{x})$ , at each position,  $\mathbf{x}$ . This is done by introducing a Lagrange multiplier (potential),  $V(\mathbf{x})$ , at each position,  $\mathbf{x}$ , and solving the following equation:

$$0 = \frac{\delta}{\delta j_{\mu}(\mathbf{x})} \left( \mathcal{E} + \int_{\Omega} d^d x V \nabla \cdot \mathbf{j} \right) = \frac{j_{\mu}(\mathbf{x})}{|j_{\mu}(\mathbf{x})|^{2-\gamma}} - \frac{\partial}{\partial x_{\mu}} V(\mathbf{x}), \quad (6)$$

where  $\mu = 1, 2, \dots, d$ . Because we expect that the CPDF does not depend on boundary conditions in the large size limit, we choose  $\mathbf{j}(\mathbf{x}) = 0$  at the boundary. We now assume that the solution depends only on  $\|\mathbf{x}\|_{\gamma}$ : because  $\mathcal{E}$  is convex, a solution with this property (if it exists) is the unique solution. Using the above choice of the input currents  $\int_{\Omega} d^d x i(\mathbf{x}) = 0$  and the conservation law  $\nabla \cdot \mathbf{j}(\mathbf{x}) = i(\mathbf{x})$ , by applying Gauss theorem one gets that the boundary condition on the volume  $\Omega$  are automatically satisfied. Equation (6) together with current conservation gives the following radial current density as the optimal solution of Eq. (5),

$$\mathbf{j}(\mathbf{x}) = \mathbf{x} \frac{i_0}{d} \left[ 1 - \left( \frac{L}{\|\mathbf{x}\|_{\gamma}} \right)^d \right]. \quad (7)$$

This solution is radially symmetric only with the metric defined in terms of the  $\gamma$  norm itself: thus the equipotential lines defined by  $\|\mathbf{j}\|_{\gamma} = \text{constant}$  are circles only for  $\gamma = 2$ , whereas when  $\gamma \rightarrow \infty$  (1) they become squares with sides parallel to the coordinate axis (45°-tilted squares). The CPDF is given by  $P_c(j|L) = |\Omega|^{-1} \int_{\Omega} d^d x \sum_{\mu} \Theta(|j_{\mu}(\mathbf{x})| - j)$  if we consider currents' components, or by

$$P_c(j|L) = |\Omega|^{-1} \int_{\Omega} d^d x \Theta(\|\mathbf{j}(\mathbf{x})\|_{\gamma} - j) \quad (8)$$

if we consider current norm [32] [ $\Theta(z) = 1$  if  $z > 0$  and zero otherwise]. It can be shown that asymptotic behaviors are the same in both cases. Using the explicit solution Eq. (7) one sees that  $P_c(j|L)$  depends only on the dimensionless ratio  $j/(i_0 L)$  for all  $d$ . When  $d = 2$  Eq. (8) takes the simple closed form:

$$P_c(j|L) = F\left(\frac{j}{i_0 L}\right), \quad F(z) = (\sqrt{1+z^2} - z)^2, \quad (9)$$

which is of the kind anticipated in Eqs. (2) and (4) with  $\tau = 3$ . The prediction Eq. (9) is shown in Fig. 4 compared to CPDFs of numerical simulations calculated considering currents' components. Even though we do not have the explicit analytical form for  $d > 2$  it is not difficult to verify the asymptotic behavior of Eq. (4). Indeed for  $j/L \gg 1$  the leading contribution in Eq. (8) comes from  $\|\mathbf{x}/L\|_{\gamma} \ll 1$  leading to  $P_c(j|L) \sim (j/L)^{(1-\tau)}$  with  $\tau = (2d-1)/(d-1)$  for  $d > 1$ . The minimum  $\|\mathbf{x}\|_{\gamma}$  is given by the underlying lattice spacing, say  $a$ , and so, according to Eq. (7), the maximum current is of order  $a i_0 (L/a)^d$ . Thus scaling holds in the region  $1 \leq j/i_0 L \lesssim (L/a)^{d-1}$ . The special case  $d = 1$  is trivial and one gets

$P_c(j|L) = 1 - 2j/(i_0 L) \Theta[1 - 2j/(i_0 L)]$ . Notice that in this case the scaling region has shrunk to zero.

The case  $\gamma < 1$  cannot be treated in the same way as above. In fact in [13] it was shown that for functional (1), with  $E(z) \propto z^\gamma$ , any current configuration, with currents being different from zero only on the bonds of a spanning tree, is a local minimum. For such solutions the second term in Eq. (6) would diverge in correspondence of the bonds not belonging to the spanning tree.

The above results can be generalized to the case of a generic convex cost function with finite first derivative as follows. While in the presence of an underlying network the natural choice for the cost function is given by Eq. (1) in the continuum there are at least two natural choices. The first choice corresponds to  $\mathcal{E} = \int_{\Omega} d^d x \sum_{\mu} E(|j_{\mu}(\mathbf{x})|)$  whereas the second one is given by

$$\mathcal{E} = \int_{\Omega} d^d x E(\|\mathbf{j}(\mathbf{x})\|_{\gamma}). \quad (10)$$

It can be shown that, although these two functionals have different optimal configurations, their CPDF have the same scaling behavior for small and large currents. For the previous case,  $E(z) = z^\gamma/\gamma$ , the two choices coincide. The minimum of the cost function, Eq. (10), in the domain  $\Omega = \{x: \|\mathbf{x}\|_{\gamma} \leq L\}$  and with the constraint of current conservation proceeds as before. The stationarity conditions of the constrained problem are

$$E'(\|\mathbf{j}(\mathbf{x})\|_{\gamma}) \frac{|j_{\mu}(\mathbf{x})|^{\gamma-2}}{\|\mathbf{j}(\mathbf{x})\|_{\gamma}^{\gamma-1}} j_{\mu}(\mathbf{x}) = V'(\|\mathbf{x}\|_{\gamma}) \frac{|x_{\mu}|^{\gamma-2}}{\|\mathbf{x}\|_{\gamma}^{\gamma-1}} x_{\mu}, \quad (11)$$

where, as before, we have assumed that the potential  $V(\mathbf{x})$  is a function of  $\|\mathbf{x}\|_{\gamma}$ . The solution is given by  $j_{\mu}(\mathbf{x}) = x_{\mu} f(\|\mathbf{x}\|_{\gamma})$  with  $V(z)$  satisfying the equation  $E'(f) = V'(z)$  (*prime* indicates the derivative with respect to the argument). Imposing current conservation we get  $f(z) = i_0/d[1 - (L/z)^d]$  leading again to solution (7). In turn this implies that the scaling behavior of the CPDF as defined in Eq. (8) is independent of the specific cost function as long as it remains convex.

#### IV. INHOMOGENEOUS CASES

We have further tested the robustness of our results by performing additional numerical simulations on systems subject to independent, equally distributed random current injection,  $i(\mathbf{x}) > 0$  at the nodes, or in the presence of nonuniform conductivity where the cost function is given by  $\mathcal{E}(\{I_b\}) = \sum_b k_b |I_b|^\gamma$  where  $k_b$  are random positive numbers.

As random distribution for injections and conductances we have chosen a power law to ensure a high degree of inhomogeneity. The simulation results of Fig. 5 show that the leading trend for large currents remains the same as in the uniform case studied above. Thus it is plausible that the scaling behavior of the current distribution corresponding to the optimal solution of the uniform case might remain the same even for the more general case of a spatially varying convex

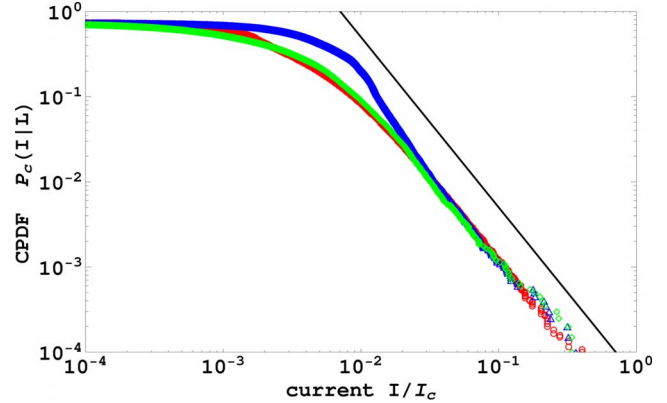


FIG. 5. (Color online) Comparison among the CPDF for the uniform case (red circles) with two examples of the heterogeneous conductivity (green rhombi) and injection cases (blue triangles) for a  $L=151$  lattice, with  $E(|I_b|) = |I_b|^\gamma/\gamma$  and  $\gamma=2$ . The probability distribution used to extract random resistances and injections is a power law with exponent  $-1.5$ , at large values, in order to provide a high degree of inhomogeneity.  $I_c$  is properly chosen to show that the power law exponent is the same at large currents for the three configurations. The shown straight line has slope  $-2$  as our analytical results predict.

cost function. These results differ from the case of random transportation dynamics [17–19] for which it was shown that the uniform injection case is equivalent to our optimization problem with  $\gamma=1$  [11]. Indeed for these models the scaling behavior of the CPDF proves sensitive to the distribution of the injections. However the present numerical results suggest that this equivalence cannot be generalized to the random injection case.

#### V. CONCLUSIONS

In summary, we have studied a class of optimal transportation networks with a convex cost function as given by Eq. (1) whose prototype is  $\mathcal{E}(\{I_b\}) = \sum_b |I_b|^\gamma$  with  $\gamma > 1$ . The optimal current configurations exhibit a probability distribution function characterized by a scaling behavior given by Eqs. (2) and (4). The scaling exponent of the current distribution proves robust with respect to (i) the choice of the transportation cost, as far as it is convex and has finite first derivatives with respect to the currents; (ii) the distribution of injected currents; (iii) position-dependent (convex) cost functions. The analytical results show that the exponent of the asymptotic power-law behavior of the current probability distribution function varies continuously from 3 in two dimensions to 2 at infinite dimensions with no evidence of an upper critical dimension.

#### ACKNOWLEDGMENTS

We are grateful to Jayanth Banavar for invaluable discussions. This work was supported by a grant of Fondazione Cassa di Risparmio 2008.

- [1] T. A. McMahon and J. T. Bonner, *On Size and Life* (Scientific American Library, New York, 1983).
- [2] L. W. Mays, *Water Distribution System Handbook* (McGraw-Hill, New York, 1999).
- [3] P. Ball, *The Self-Made Tapestry: Pattern Formation in Nature* (Oxford University Press, Oxford, 1998).
- [4] I. Rodriguez-Iturbe and A. Rinaldo, *Fractal River Basins: Chance and Self-Organization* (Cambridge University Press, New York, 1997).
- [5] G. Caldarelli, *Scale-Free Networks: Complex Webs in Nature and Technology* (Oxford University Press, New York, 2007).
- [6] R. Albert and A. L. Barabási, *Rev. Mod. Phys.* **74**, 47 (2002).
- [7] A. L. Barabási, *Linked: How Everything Is Connected to Everything Else and What It Means for Business, Science, and Everyday Life* (Plume Books, New York, 2003).
- [8] J. R. Banavar, F. Colaiori, A. Flammini, A. Maritan, and A. Rinaldo, *J. Stat. Phys.* **104**, 1 (2001).
- [9] P. G. Doyle and J. L. Snell, *Random Walk and Electric Networks* (American Mathematical Society, Providence, 1989).
- [10] J. P. Straley and S. W. Kenkel, *Phys. Rev. B* **29**, 6299 (1984).
- [11] A. Maritan, F. Colaiori, A. Flammini, M. Cieplak, and J. R. Banavar, *Science* **272**, 984 (1996).
- [12] A. Maritan, A. Rinaldo, R. Rigon, A. Giacometti, and I. Rodriguez-Iturbe, *Phys. Rev. E* **53**, 1510 (1996).
- [13] J. R. Banavar, F. Colaiori, A. Flammini, A. Maritan, and A. Rinaldo, *Phys. Rev. Lett.* **84**, 4745 (2000).
- [14] I. Rodriguez-Iturbe *et al.*, *Water Resour. Res.* **28**, 1095 (1992); *Geophys. Res. Lett.* **19**, 889 (1992); A. Rinaldo *et al.*, *Water Resour. Res.* **28**, 2183 (1992); A. Rinaldo, I. Rodriguez-Iturbe, R. Rigon, E. Ijjasz-Vasquez, and R. L. Bras, *Phys. Rev. Lett.* **70**, 822 (1993).
- [15] T. M. Liggett, *Interacting Particle Systems* (Springer, Berlin, Heidelberg, 2005).
- [16] M. R. Swift, F. Colaiori, A. Flammini, A. Maritan, A. Giacometti, and J. R. Banavar, *Phys. Rev. Lett.* **79**, 3278 (1997).
- [17] H. Takayasu, I. Nishikawa, and H. Tasaki, *Phys. Rev. A* **37**, 3110 (1988).
- [18] H. Takayasu, M. Takayasu, A. Provata, and G. Huber, *J. Stat. Phys.* **65**, 725 (1991).
- [19] H. Takayasu, M. Takayasu, and Y.-H. Taguchi, *Int. J. Mod. Phys. B* **8**, 3887 (1994).
- [20] D. Dhar, *Phys. Rev. Lett.* **64**, 1613 (1990).
- [21] J. R. Banavar, A. Maritan, and A. Rinaldo, *Nature (London)* **399**, 130 (1999).
- [22] M. Durand, *Phys. Rev. Lett.* **98**, 088701 (2007); *Phys. Rev. E* **73**, 016116 (2006); M. Durand and D. Weaire, *Phys. Rev. E* **70**, 046125 (2004).
- [23] S. Bohn and M. O. Magnasco, *Phys. Rev. Lett.* **98**, 088702 (2007).
- [24] B. L. Golden, *Networks* **5**, 331 (1975).
- [25] L. De Michele and P. M. Soardi, *Proc. Am. Math. Soc.* **109**, 461 (1990).
- [26] W. Millar, *Philos. Mag.* **42**, 1150 (1951).
- [27] F. Colaiori, A. Flammini, A. Maritan, and Jayanth R. Banavar, *Phys. Rev. E* **55**, 1298 (1997).
- [28] J. Shewchuk, *An Introduction to the Conjugate Gradient Method without the Agonizing Pain, Technical Report* (School of Computer Science, Carnegie Mellon University, Pittsburgh, 1994).
- [29] A. Clauset, C. R. Shalizi, and M. E. J. Newman, e-print arXiv:0706.1062.
- [30] M. E. J. Newman, *Contemp. Phys.* **46**, 323 (2005).
- [31] B. Efron, *SIAM Rev.* **21**, 460 (1979).
- [32] It can be easily shown that if we define the CPDF with reference to a generic norm  $\|\cdot\|_\alpha$  the asymptotic behavior at large currents remains unchanged.